*metals*

MDPI

*Review*

# Influence of Cryogenic Temperatures on the Microstructure and Mechanical Properties of Magnesium Alloys: A Review

**Hajo Dieringa**

Helmholtz-Zentrum Geesthacht, Centre for Materials and Coastal Research, MagIC—Magnesium Innovation Centre, Max-Planck-Str. 1, 21502 Geesthacht, Germany; hajo.dieringa@hzg.de; Tel.: +49-4152-871955

Academic Editor: Manoj Gupta
Received: 14 November 2016; Accepted: 24 January 2017; Published: 30 January 2017

**Abstract:** Magnesium alloys have been used in the automotive industry and 3C (computer, communication, and consumer electronics) for many years. Their room temperature properties combined with their low density offer a wide range of applications, especially when processed by High Pressure Die Casting (HPDC). The use of magnesium alloys at higher temperatures is well-studied; special creep resistant alloys containing the rare earth elements silver or yttrium are needed. However, when it comes to very low temperatures, only a few studies have been performed to determine the property-microstructure relationship. The possible fields of application at low temperatures are aerospace and satellite parts and tanks for liquefied gases. This review shall not only examine mechanical properties at low temperatures, but also the permanent effects of cyclic or long-lasting cryogenic treatment on the microstructure and mechanical properties. It was found that cryogenic treatment is able to influence the precipitate concentration and grain orientation in some magnesium alloys. Reduction in the number of brittle phases is improving ductility in some cases. It is well-known that high speed tool steels, in particular, can be influenced by cryogenic treatment. Whether this is possible with magnesium alloys and what the mechanisms are shall be reviewed.

**Keywords:** magnesium alloys; low temperature; DCT (Deep Cryogenic Treatment); aerospace; mechanical properties; cryogenic

## 1. Introduction

Magnesium alloys are widely used in automotive applications, 3C (computer, communication, and consumer electronics), tools, and to some extent in aerospace and aeronautics. Their main advantage is low density. Aluminum alloys with a density of ~2.8 g/cm$^3$ are 50% heavier compared with magnesium alloys having a density of ~1.8 g/cm$^3$. The low density of magnesium alloys has a significant economic savings effect and this is especially true in the aerospace and aeronautic industries. Here, the use of magnesium casting alloys for pumps, housings, accessories, and hardware for the handling of liquefied gases is of interest. Magnesium wrought alloys in sheets or extrusions may be used for tanks of liquefied gases, extruded ribs, and connectors [1].

Most of the magnesium alloys have been developed and used with High Pressure Die Casting (HPDC). They contain a minimum of 4 wt. % Al to improve their castability and several other alloying elements to improve their corrosion properties, strength, and creep resistance. There are only a few magnesium alloys for wrought applications in the market. AZ31 is the most widely investigated alloy, but AZ80 and ZE10 are also used. Magnesium alloys, in general, suffer from low deformability even at room temperature (RT) resulting from their hexagonal close-packed (HCP) crystal structure. Whereas at RT, mainly basal and prismatic slip <a> and twinning are the active deformation modes;

at temperatures above 220 °C <a+c> slip also takes place. Twinning mainly takes place at {10–11}, {10–12}, and {10–13} planes at low temperatures and at higher strain rates [2,3] which are needed to satisfy the von Mises yield criterion for unrestricted plastic deformation. These twinning effects may also act as a trigger for brittle fracture and enhance micro-cracks, which are undesired effects in structural materials [4].

This review paper will not only describe the material properties tested at low temperatures, but also mention the changes in mechanical properties after magnesium alloys have been exposed to cryogenic temperatures. Both cases are of interest to understand the low temperature applications of magnesium alloys and the influence of low temperatures on microstructural features.

## 2. Cryogenic Treatment of Magnesium Alloys

Cryogenic treatment (CT) is a process that aims to modify metallic materials in order to improve their mechanical properties. Usually there is a distinction between CT at below zero temperatures and deep cryogenic treatment (DCT) at temperatures of 77 K and below. The temperature of liquid nitrogen at ambient pressure is 77 K. An overview is given in [5]. CT has mainly been used with steels, such as high speed steels, to improve their hardness or wear resistance [6,7]. CT promotes the transformation of the retained austenite into martensite and additionally precipitates very fine carbides.

In [8], the authors describe their investigations with hot rolled AZ31 sheets (Mg-3Al-1Zn-0.2Mn). Specimens were cut and cryogenically treated at 77 K with a cooling speed of 2 K/min for a soaking time of 2, 4, 24, and 48 h. After soaking, the specimens were slowly heated to room temperature. Microstructure investigations show that CT leads to more twinning, in combination with a change in grain orientation, compared to that of the untreated samples. Hardness and tensile strength are higher compared to that of untreated samples, but highly depend on the soaking time. The same authors performed cycling CT on magnesium alloy AZ91 as well [9]. Each cycle included an 8 h holding at 200 °C, followed by progressively cooling over 6 h to −180 °C and holding at this temperature for 2 h. Hardness increased after three cycles by 65.7% and corrosion resistance improved as well. An increase in β-phase content ($Mg_{17}Al_{12}$) and its uniform distribution is assumed to cause this improvement.

Bhale et al. investigated the influence of deep cryogenic treatment on squeeze cast magnesium alloy AE42 [10]. DCT was done in liquid nitrogen for 4, 8, and 16 h at −196 °C (77.15 K). The volume fraction of α-Mg and $Al_4RE$ phases in the microstructure of AE42 changed significantly with the length of time of DCT. The amount of α-Mg increases with duration of DCT whereas the amount of $Al_4RE$ decreases. Strength and ductility development against duration of DCT are shown in Figure 1. The decreasing yield strength over the duration of DCT is marginal, whereas ultimate tensile strength (UTS) and ductility increase significantly. This is attributed to the dissolution of the brittle $Al_4RE$ phase. Creep tests and wear and hardness tests were also performed and it could be shown that creep, wear resistance, and hardness decreased with the duration of DCT. That is also attributed to the loss of the $Al_4RE$ phase. Corrosion tests have also shown that with decreasing numbers of $Al_4RE$ phases, the corrosion resistance decreases.

Magnesium alloy AZ91 was processed in High Pressure Die Casting (HPDC) followed by a T6 heat treatment (solution heat treatment followed by artificially aging) [11]. DCT of some samples was done before aging. Both materials were compared with regard to microstructure and mechanical properties, and it was found that ductility increases slightly when DCT is done. The ultimate tensile strength remains the same, but yield strength decreases slightly. The DCT causes a decrease in grain size in addition and an increase in continuous precipitation, which may cause the same UTS of T6 and DCT + T6 materials.

Again, AZ91 was investigated in terms of microstructure, creep, and wear resistance after DCT [12]. The materials were cast at 750 °C melt temperature in steel molds heated to 300 °C. After DCT, the yield strength of the AZ91 samples was slightly higher, 98 MPa compared to 91 MPa in the as-cast state, and the ultimate tensile strength increased after DCT from 170 MPa to 187 MPa. The hardness was also improved by DCT, from 59 BHN to 67 BHN. The reason for strengthening is due to a change in morphology of the β-phase. A more coarsely divorced β-phase appeared after DCT. From creep tests it could be shown that the minimum creep rate decreased drastically after DCT. The calculated stress exponents and activation energies illustrated a change from a mixed mode with some grain boundary effects in the as-cast AZ91 to a dislocation climb controlled creep in the DCT materials. Especially at higher loads, the wear resistance of the DCT materials improved significantly compared to that of the as-cast AZ91.

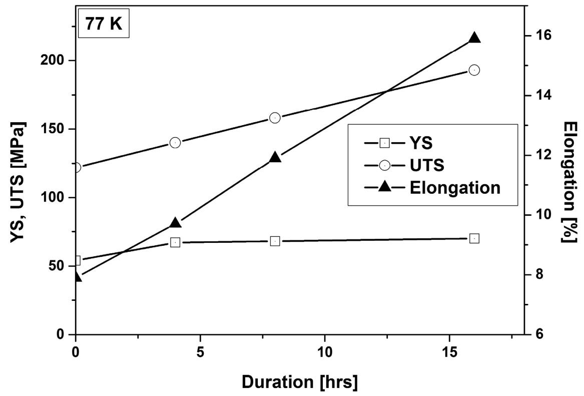


**Figure 1.** Yield strength (YS), ultimate tensile strength (UTS), and elongation to fracture of AE42 against deep cryogenic treatment (DCT) duration (redrawn after Figure 5 in [10]).

AZ91 ingots were melted and quenched in air, water, and by DCT [13]. Some of the samples were aged, some put away without ageing, and some were treated with DCT. Samples from this 3 × 3 matrix were tested in terms of microstructure, hardness, and wear resistance. It was found that the higher the cooling power during quenching, the higher the amount of β-phase in the matrix. The highest rate was from water cooling; even though liquid nitrogen is much colder, it does not have the ability to remove heat as fast as water cooling does. A further DCT improved the hardness and wear resistance. It is assumed that the structural contraction during DCT causes aluminum atoms to jump to nearby defects and act as preferential sites for nucleation of the β-phase.

In two subsequent papers, Liu et al. described the wear and mechanical properties of an Mg-1.5Zn-0.15Gd (at. %) [14,15]. The material was extruded, cut, and then immersed in liquid nitrogen for between 2 and 24 h followed by reheating to room temperature in air. Material without DCT was retained for comparison. Microstructural observation showed that the amount of W phase in the matrix increased with DCT duration from 3.6% to 7.8% after 24 h of DCT. As well as the amount of the W phase, the micro hardness increased from 52 ± 2 to 60 ± 2 HV. The wear resistance of cryogenically treated Mg-1.5Zn-0.15Gd magnesium alloy improved significantly with increased duration of DCT. The wear rate and friction coefficient decreased with increased duration of DCT. The refinement of the W phase and its increase in volume fraction was attributed to this behavior. In tensile tests, it was shown that ductility increases significantly from 8.6% to 15.4% after 24 h of DCT, which is attributed to the development of the W phase with an increased duration of treatment. Ref. [15] concludes with the assumption that due to the contraction of the samples during the DCT, only precipitates that have a much lower atomic density compared to that of α-Mg can be formed. This criterion is assumed to be guidance for further use and development of DCT on magnesium alloys for strengthening by developing precipitates.

After only a few years, magnesium alloys are again the focus of interest, this time for biomedical applications. They may be used as degradable implants, for which a second operation to remove them is not necessary. It reduces suffering for the patients and saves money. Wrought magnesium alloy ZK60 (Mg-5.67Zn-0.52Zr-0.012Mn) rods were turned in dry conditions and under a flow of liquid nitrogen [16]. The turning parameters were detected and surface roughness was measured. The cutting temperature was significantly reduced, which is only to be expected. Depending on the feed rate, temperature increases with increasing cutting speed, and the temperature was between 110 °C and

140 °C; whereas in liquid nitrogen, it was cooled down to between 40 °C and 55 °C. The surface roughness after turning in liquid nitrogen was reduced by 25% to 40% compared to that in dry turning. This effect is due to a cushion of lubricant between the contact surfaces. An increased intensity of basal planes at the surface was found, and this seems to be the reason for improved micro hardness.

## 3. Mechanical Properties at Cryogenic Temperatures

Two magnesium alloys, ZK60 (Mg-4.9Zn-0.49Zr) and AZ31 (Mg-2.5Al-0.092Zn-0.37Mn), were tested mechanically in the temperature range of 123 K to 296 K [4]. ZK60 materials were extruded at 593 K followed by heat treatment for 2 h at 775 K. The resulting average grain size was 30 µm. AZ31 was examined in the form of a rolled plate prepared by cross rolling at 825 K. The plate was annealed for 1 h at 620 K, and the resulting average grain size was 50 µm.

The mechanical properties of ZK60 at low temperatures are shown in Figure 2. From microstructural analysis it was concluded that the deformation behavior followed a sequential transition, initially from slip mechanisms that control the parabolic strain-hardening region (decreasing the strain hardening rate) to a mechanical twinning propagation that controls the linear strain hardening stage (constant strain hardening rate). Even though a low temperature regime was applied, the ZK60 alloy behaves in a ductile manner, without any significant features of brittleness, neither in ductility nor in fracture mode. In ZK60 the rate controlling deformation mechanism changes from slip dominated at 296 K to twinning dominated at lower temperatures. It is assumed that the yield stress for slip is lower than that for uniform twinning in the whole range of test temperatures. Whereas the transition strain decreases with decreasing temperature, the slip/twinning transition stress is almost insensitive to test temperatures.

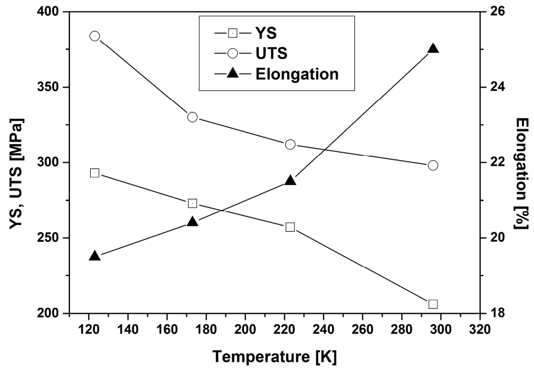


**Figure 2.** Temperature dependence of the tensile properties of ZK60 (after [4]).

The AZ31 sheets were evaluated in terms of fracture toughness depending on rolling direction. According to the ASTM E399 standard, specimens were taken from a sheet in T-L, L-T, T-S, and L-S directions respectively, where L is the longitudinal or rolling direction, T is the transverse direction, and S is the thickness of the sheet. Fracture toughness Kc is summarized in Table 1 and it can be clearly seen that toughness in the L-T direction is higher than in the T-L direction.

**Table 1.** Fracture toughness [MPa·m$^{1/2}$] as a function of temperature and orientation (L: longitudinal or rolling direction, T: transverse direction, and S: thickness of the sheet) [4].

| Temperature [K] | Crack Plane Orientation | | | |
|---|---|---|---|---|
| | **T-L** | **L-T** | **T-S** | **L-S** |
| 296 | 9.5 | 14.3 | N/A | N/A |
| 200 | 10.5 | N/A | N/A | N/A |
| 173 | 10.1 | 15.5 | 8.6 | 9.5 |
| 123 | 9.5 | 10.2 | 7.0 | 10.1 |

Several aluminum and magnesium alloys were tested in [17] at low temperatures for their tensile strength and fatigue. Only magnesium alloys are discussed here, and their compositions are given in Table 2. Concerning the temperature range 20 to 293 K, the alloy VM12 shows the best combination of mechanical properties. Magnesium alloy MI10 also shows satisfactory properties, see Figure 3.

**Table 2.** Composition of magnesium alloys investigated in [17].

| Alloy | Al | Mn | Zn | Zr | Nd | In | Mg |
|---|---|---|---|---|---|---|---|
| MI5 | 7.5 | 0.23 | 0.59 | - | - | - | Bal. |
| MI12 | - | - | 4.5 | 0.8 | - | - | Bal. |
| MI10 | - | - | 0.22 | 0.57 | 2.53 | - | Bal. |
| VM12 | - | - | - | 0.48 | 2.3 | 0.4 | Bal. |

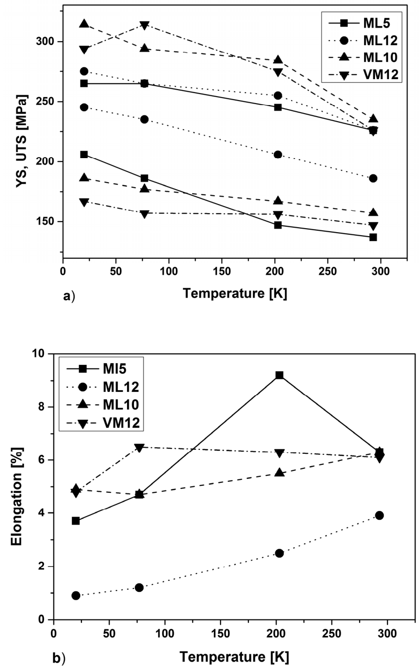


**Figure 3.** (**a**) Temperature dependent yield strength (YS) and ultimate tensile strength (UTS); and (**b**) temperature dependent elongation to fracture (after [17]).

Magnesium alloy AZ31B in three different heat treatment conditions was tensile tested at 4.2 K, 77 K, 200 K, and 300 K [18]. The material shows no yielding points at 4.2 K and 77 K, but the increase in ultimate tensile strength (UTS) of over 60% is quite significant (see Table 3). An explanation for the strengthening effect at low temperatures is that in AZ31B the aluminum and zinc atoms are the main strengthening agents. At higher temperatures, both have a large solid solubility in magnesium. This solubility is reduced at low temperatures, and a fine distributed second phase forms in the matrix, which strengthens the alloy. Electrical resistivity has been measured at low temperature, but the effect in AZ31B is negligible. Thermal conductivity decreases with decreasing temperature. At room temperature it is approximately 28 W/mK, and at 77 K it goes down to 14 W/mK.

**Table 3.** Tensile properties of AZ31B magnesium alloy [18].

| Temperature [K] | UTS [MPa] | YS [MPa] | Elongation [%] |
|---|---|---|---|
| 300 | 217 | 132 | 9.9 |
| 77 | 282 | - | 4.5 |
| 4.2 | 366 | - | 4.5 |

In [19], several pure metals were investigated to determine their fatigue properties at low temperatures. Only the results of pure magnesium (99.98%) are described here. Fatigue tests were done at 4.2, 20, 90, and 293 K using liquid oxygen, hydrogen, and helium in direct contact with the specimens. Figure 4 shows the curves of peak stress against the number of cycles before fracture for magnesium. It can be seen that there is little difference between 4.2 and 20 K, but compared to room temperature, there is a considerable increase in fatigue strength at low temperatures.

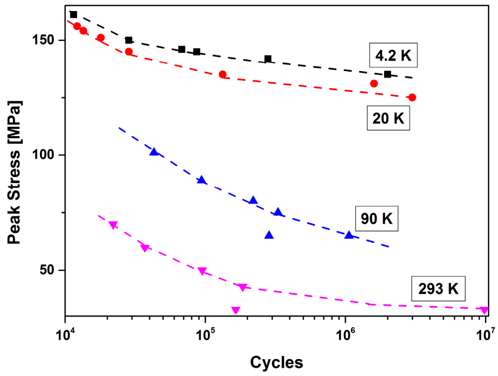


**Figure 4.** Peak stress against number of cycles before fracture at 4.2, 20, 90, and 293 K (redrawn from Figure 88 in [19]).

A report by NASA (National Aeronautics and Space Administration) compares the mechanical properties at low temperatures of 29 alloys [20]. These included aluminum, titanium, nickel, and magnesium alloys, as well as some steels. Tests were performed on sheets at temperatures between room temperature and 5.3 K. Two magnesium-lithium alloys were investigated. The compositions of LA91 and LA141 are given in Table 4. It is mentioned that alloying magnesium with lithium reduces density and improves the ductility of hcp-magnesium. Up to 5.7% Li can be dissolved in α-Mg. A β-phase with body-centered cubic (BCC) structure appears with Li content between 5.7% and 10.3%. Above 10.3%, a perfect BCC structure is obtained. Figure 5 shows the mechanical properties of these alloys. LA91 exhibits higher strength compared to LA141. Ductility in all cases remains good, even at very low temperatures, with a minimum at 200 K.

**Table 4.** Composition of magnesium-lithium alloys.

| Alloy | Li | Al | Mg |
|---|---|---|---|
| LA91 | 9.0 | 1.0 | Bal. |
| LA141 | 14.5 | 1.5 | Bal. |

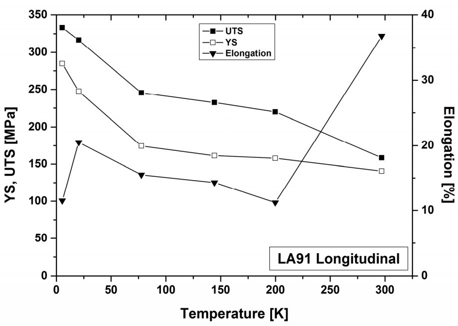


(**a**)

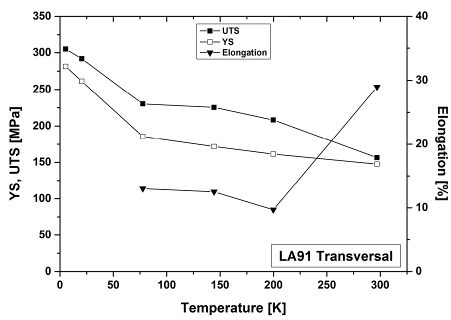


(**b**)

**Figure 5.** *Cont.*

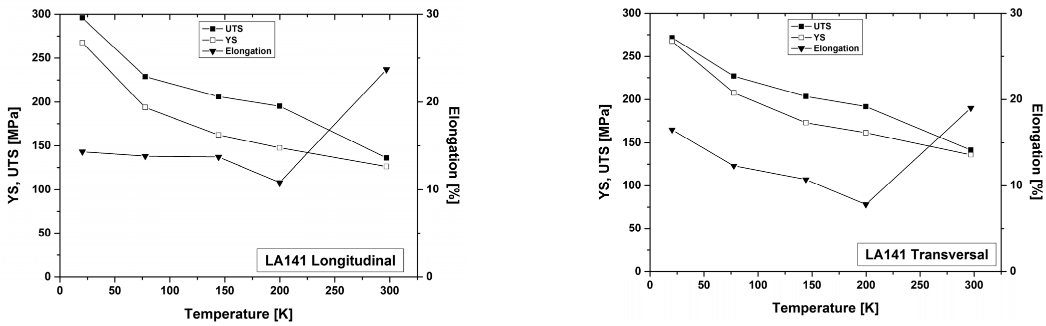


(c) (d)

**Figure 5.** Tensile properties of magnesium alloys, LA91 in (**a**) and (**b**) and LA141 in (**c**) and (**d**), in longitudinal and transverse direction (redrawn from [20]).

The first evaluation of low temperature properties for a large matrix of magnesium alloys was determined in another NASA report [21]. Matrix I did not show satisfying properties and was replaced by matrix IA. After the alloys were cast, it was found that neither zirconium nor silicon act as grain refiners in alloys containing more than 7% lithium. Alloys containing aluminum were grain refined with hexachlorobenzene. After mechanical testing of large numbers of different alloy systems containing lithium, zirconium, aluminum, thorium, zinc, manganese, silver, and cadmium, three alloys were selected for further testing, as given in Table 5.

After several tests, the rolling temperature was chosen to be 126 °C. With alloy II4, a solution heat treatment was done at 315 °C for 1 and 3 h. UTS and elongation after aging is plotted in Figures 6a and 6b, respectively. Tensile tests of all alloys at cryogenic temperatures were performed and the results are shown in Figure 7 for alloys II4, IA6, and ZLH972. A similar trend can be seen for yield strength and ultimate tensile strength. Both show a slight increase with decreasing temperature. Ductility goes down with temperature, as expected.

**Table 5.** Composition of best alloys selected in [21].

| Alloy | Al | Zn | Mn | Th | Zr | Li | Cd | Ag |
|---|---|---|---|---|---|---|---|---|
| II4 | - | 6.0 | - | 3.0 | 1.0 | 7.0 | 5.0 | 6.0 |
| IA6 | 4.0 | 2.0 | 1.0 | 3.0 | - | 9.0 | - | 4.0 |
| ZLH972 | - | 9.0 | - | 2.0 | - | 7.0 | - | - |

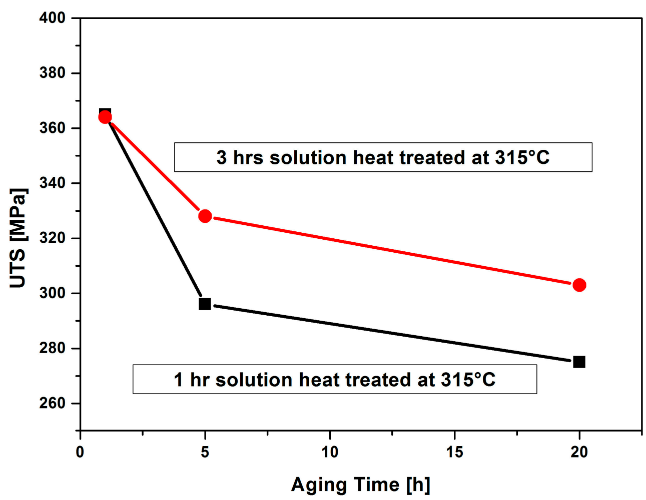


(a)

**Figure 6.** *Cont.*

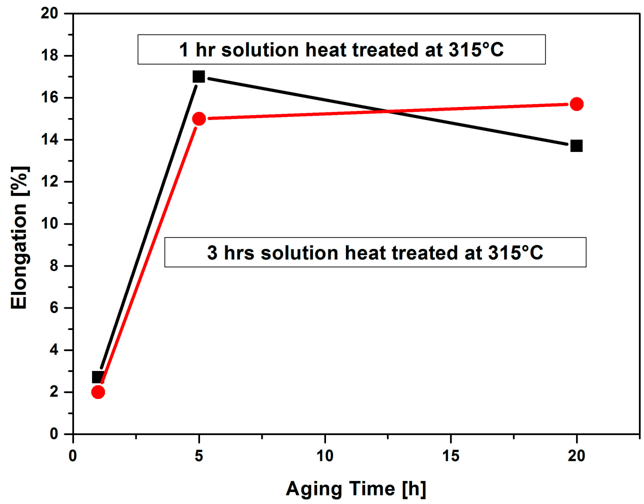


(**b**)

**Figure 6.** Effects of aging time on a) UTS and b) elongation to fracture of alloy II4 (after [21]).

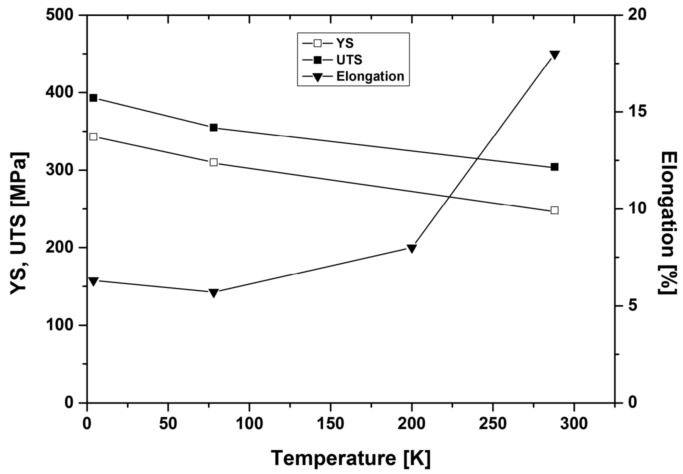


(**a**)

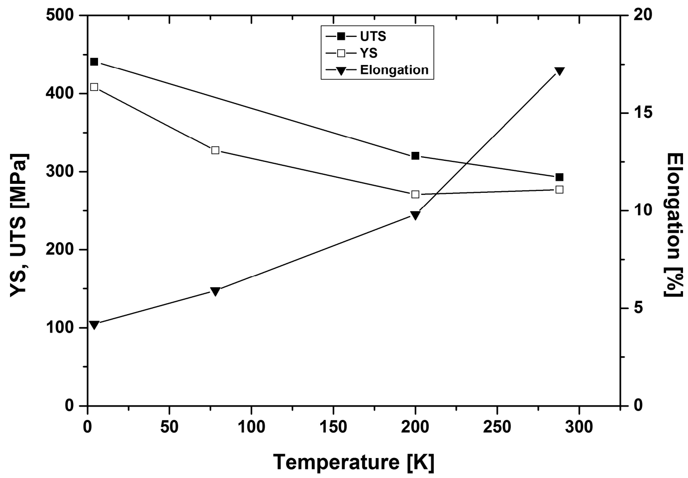


(**b**)

**Figure 7.** *Cont.*

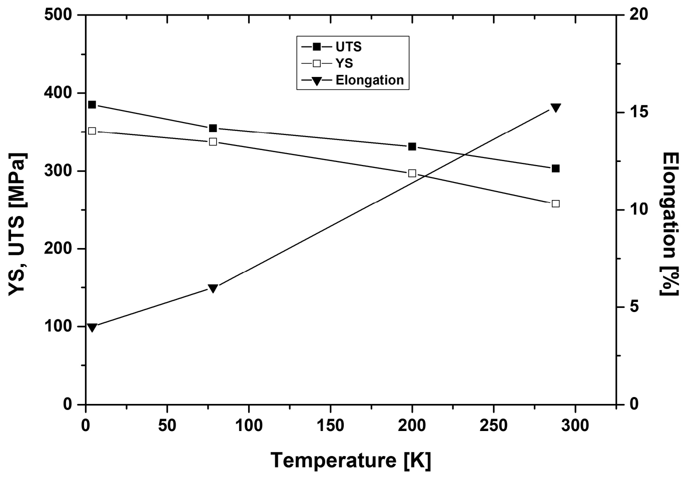


(**c**)

**Figure 7.** Mechanical properties of alloys (**a**) II4; (**b**) IA6; and (**c**) ZLH972 at low temperatures (after [21]).

A NASA Technical Memorandum describes the investigation into a magnesium alloy, ZM21, processed in sheets and tested in rolling and perpendicular to rolling directions [22]. The composition of ZM21 is given in Table 6. Under all tensile tests, the ultimate tensile strength and the yield strength is higher in the transverse direction compared to that of the longitudinal direction. There is a sharp increase in ductility between −17.8 °C and 93 °C, which results in an elongation above 45%. UTS, yield strength (YS) and elongation behavior as a function of temperature is shown in Figure 8.

**Table 6.** Composition of ZM21 [22].

| **Zn** | **Mn** | **Si** | **Fe** | **Sn** | **Pb** | **Cu** | **Ni** | **Mg** |
|---|---|---|---|---|---|---|---|---|
| 1.65 | 1.20 | <0.03 | <0.01 | <0.01 | <0.02 | <0.001 | <0.001 | Bal. |

In order to simulate the environmental conditions for satellites or other spacecraft equipment, materials were subjected to thermal cycling between cryogenic and moderately elevated temperatures under a constant load [23]. Magnesium alloys AZ91B (Mg-2.5Al-0.7Zn-0.2Mn) and HK31A (Mg-2.5-4Th-0.45-1Zr-0.15Mn) in sheet form were put under a constant stress while a current heated up the specimen immersed in liquid nitrogen for immediate cooling as soon as the current stopped. Cycling between 77 K and 588 K under constant load, counting the numbers of cycles to failure, were performed, and deformation against time curves were obtained. It was found that the number of cycles to failure increases with a decreasing nominal applied stress. An increase in maximum cycling temperature decreases the nominal stress for an equal number of cycles to failure. Magnesium alloys present only small effects of the heating rate on creep properties and failure occurrence.

Fenn mentions another reason to determine the properties of magnesium alloys at cryogenic temperatures: the use of liquefied gases in missiles as fuel [1]. In this paper, several magnesium alloys are investigated in the as-cast state, sheets, and extrusions, see Table 7. The mechanical properties of cast alloys at 77, 194, 279, 366, and 422 K are shown in Figure 9. QE22A in the T6 state presents the highest ultimate tensile strength with a moderate elongation, whereas ZH62A-T6 has the highest yield strength at 77 K, while HK31A has the highest elongation at that low temperature with 6.7%. The changes in elongation below room temperature are relatively small.

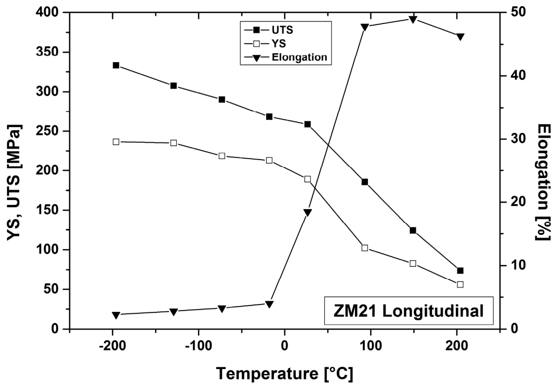


(**a**)

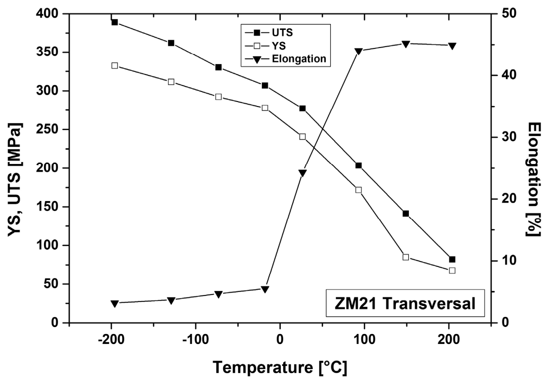


(**b**)

**Figure 8.** Mechanical properties of ZM21 sheets in (**a**) longitudinal and (**b**) transversal directions (redrawn from [22]).

**Table 7.** Chemical composition of casting alloys, sheet alloys, and extrusion alloys [1].

| Alloy | ASTM Heat Treatment | Al | Mn | Zn | Zr | Th | RE | Ag |
|---|---|---|---|---|---|---|---|---|
| | | | | Casting Alloys | | | | |
| AZ91C | T6 | 8.55 | 0.2 | 0.76 | - | - | - | - |
| AZ92A | T6 | 9.5 | 0.2 | 2.01 | - | - | - | - |
| EZ33A | T5 | - | 0.33 | 2.77 | 0.68 | - | 3.32 | - |
| HK31A | T6 | - | 0.43 | - | 0.84 | 2.99 | - | - |
| QE22A | T6 | - | 0.03 | - | 0.7 | - | 2.08 | 2.46 |
| ZH62A | T5 | 0.057 | 5.46 | 0.87 | 1.79 | - | - | - |
| | | | | Sheet Alloys | | | | |
| AZ31B | H24 | 2.9 | 0.44 | 0.94 | - | - | - | - |
| HK31A | H24 | - | 0.05 | - | 0.95 | 2.64 | - | - |
| HK31A | O | - | 0.059 | - | 0.63 | 2.95 | - | - |
| HM21A | T8 | - | 0.47 | - | - | 2.48 | - | - |
| ZE10A | O | - | 0.087 | 1.16 | - | - | 0.17 | - |
| ZE10A | H24 | - | 0.087 | 1.16 | - | - | 0.17 | - |
| | | | | Extrusion Alloys | | | | |
| ZK60A | T5 | - | - | 5.5 | 0.55 | - | - | - |
| AZ31B | F | 3.0 | - | 1.0 | - | - | - | - |
| AZ61A | F | 6.5 | - | 1.0 | - | - | - | - |
| HM31A | T5 | - | 1.9 | - | - | 3.12 | - | - |

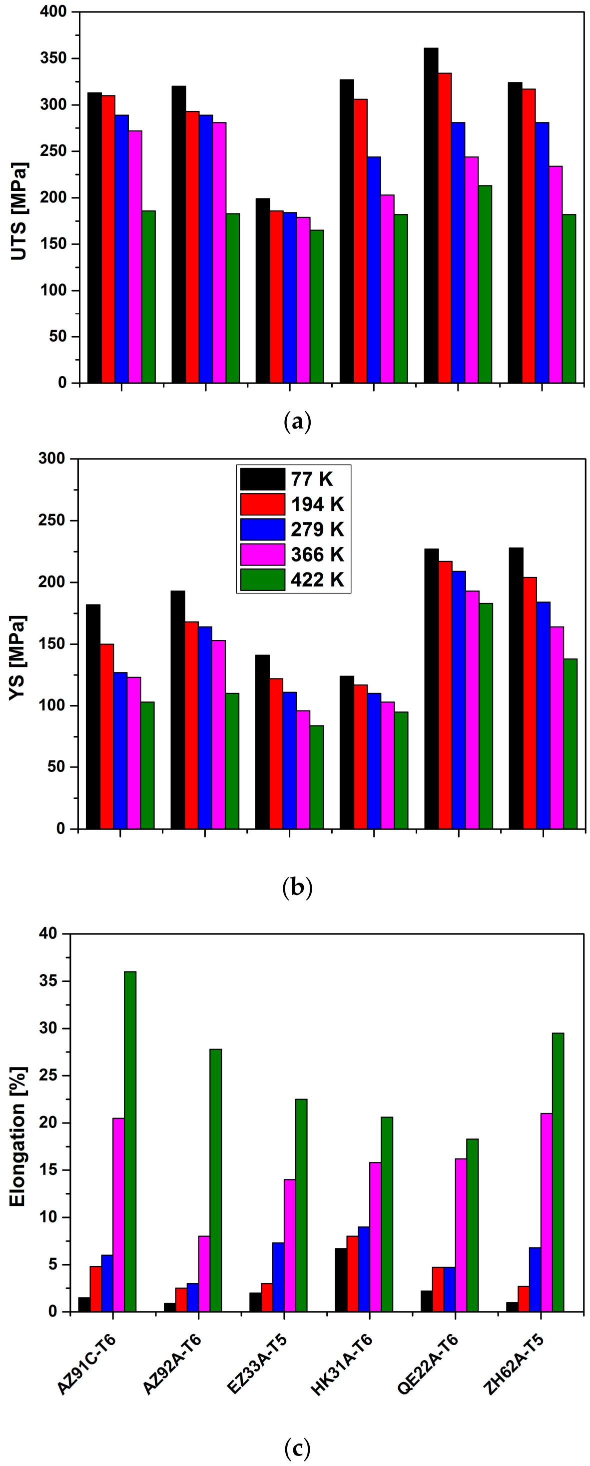


**Figure 9.** (**a**) UTS, (**b**) Yield strength, and (**c**) elongation of cast magnesium alloys at 77, 194, 279, 366, and 422 K (redrawn after [1]).

Charpy impact tests were also done at 77, 194, and 279 K. HK31A-T6 and QE22A-T6 exhibit the highest impact strength in un-notched-bar tests, and HK31A-T6 exhibits the best results in notched-bar tests. Among the sheet alloys, AZ31B-H24 alloy exhibits the highest UTS at 77 K (400 MPa). Extruded alloys were tested and it was found that ZK60A-T5 shows the highest strength and lowest elongation at 77 K, while HM31A-T5 has the lowest strength but highest elongation. Comparing all the results in [1], it can be said that although a decrease in elongation could be observed with decreases in temperature, no precipitous drop occurs when the temperature is decreased from room temperature to 77 K.

Investigations of Tang et al. include deformation and failure behavior of magnesium alloy AZ80 (Mg-8.6Al-0.56Zn-0.23Mn) in the temperature range from 77 K to 298 K [24]. The yield strength, ultimate strength, and elongation were measured. The material was tested in as-cast and extruded states. Figure 10 shows the temperature dependence of the mechanical properties. Yield strength and ultimate tensile strength increases with decreasing temperature, and elongation decreases. Especially in the range 143 K–213 K, there is a significant reduction in elongation, which is considered to be a ductile-to-brittle transition. TEM and SEM analysis showed that twinning plays an important role in deformation of AZ80 at cryogenic temperatures. The crack initiation and twinning behavior changes with decreasing temperature.

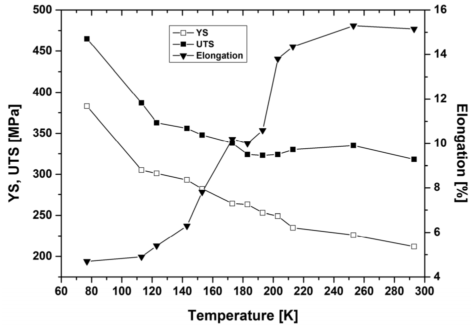


**Figure 10.** Temperature dependence of mechanical properties of AZ80 magnesium alloy (redrawn after [24]).

A rolled sheet made of AZ31 magnesium alloy was tested for tensile strength in the temperature range between 77 K and room temperature at three different strain rates [25]. The test temperatures were 77, 123, 173, 223, 273, and 300 K, applying strain rates of $10^{-4}$/s, $10^{-3}$/s, and $10^{-2}$/s. Figure 11 shows the mechanical properties of the AZ31 sheets tested. After analyzing the data according to dislocation theory, the main conclusions are that the strength of AZ31 increases with decreasing temperature, and the elongation, even at 77 K, is 5%, which is still a remarkable ductility. With deceasing temperature, the work hardening rate increases from 4.0 GPa at 300 K to 5.26 GPa at 77 K. The calculated activation volume was above 173 K between 100 and 175 $b^3$, whereas below 173 K it was much smaller. At 77 K, it was 24 $b^3$. The activation energy was approximately 160 kJ/mol above 173 K and about 20 kJ/mol below 173 K. It was found that the deformation mechanisms change at 173 K. Below this temperature the dislocation motion is controlled by interaction with the local lattice, whereas above 173 K the rate controlling mechanism is interaction with forest dislocation.

In several papers, Russian researchers investigated fatigue behavior of magnesium alloys at low temperatures [26–30]. The composition of the investigated magnesium alloys is given in Table 8, with the mechanical properties at room temperature and −135 °C in Table 9. In the first paper, only the alloy MA12 was tested [26], which is comparable to EZ31, and it was found that with decreasing temperature, the endurance increases in tests with identical cycling loading. The fatigue limit increases for annealed MA12. At both temperatures, the failure takes place intragranularly. A variation of temperature from 20 °C to −120 °C does not change the fracture toughness. Tests performed in [28] show different behavior of fatigue crack growth depending on the stress intensity factor. Two groups of alloys behave differently: MA2-1, MA15, and MA12 show two regions divided by one kink point, being independent of temperature, whereas the alloys IMV6 and MA21 have two kink points, slightly increasing with decreasing temperature. Total fatigue life $N_0$, and length of fatigue microcrack initiation period $N_i$, and the ratio of $N_i$ to $N_0$ are given in Table 10. MA2-1 and IMV6 alloys exhibit the highest resistance to fatigue crack initiation and crack growth at both temperatures 20 °C and −135 °C. MA21 and MA12 exhibit the lowest resistance under identical conditions.

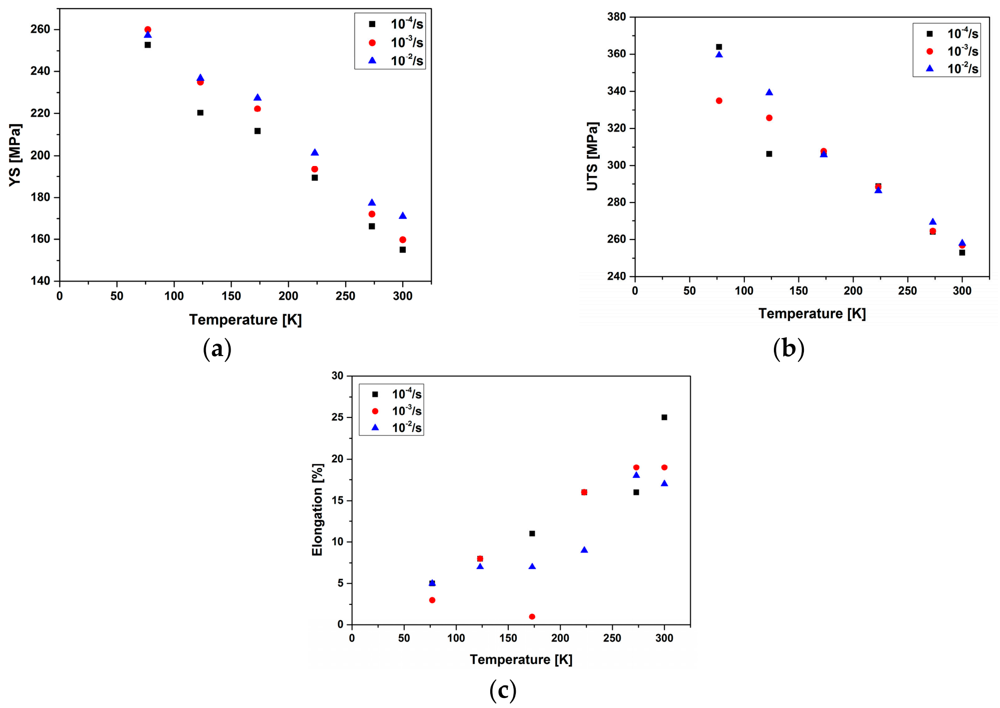


**Figure 11.** Temperature-dependent (**a**) yield strength, (**b**) ultimate tensile strength, and (**c**) elongation to fracture of AZ31 sheets (plotted after [25]).

**Table 8.** Composition of magnesium alloys tested in [26–30].

| Alloy | Al | Zn | Mn | Nd | Zr | Li | Ca | La | Y | Ce |
|---|---|---|---|---|---|---|---|---|---|---|
| IMV6 | 0.12 | - | 0.55 | - | - | - | 0.49 | - | 7.8 | 0.11 |
| MA2-1 | 4.17 | 0.85 | 0.5 | - | - | - | - | - | - | - |
| MA15 | - | 3.15 | - | - | - | - | 1.88 | 0.83 | - | - |
| MA12 | - | - | - | 2.9 | 0.44 | - | - | - | - | - |
| IMV2 or MA21 | 5.4 | 1.0 | - | - | - | 8.6 | 4.7 | - | - | - |

**Table 9.** Mechanical properties at room temperature and −135 °C [28].

| Alloy | Room Temperature | | | −135 °C | | |
|---|---|---|---|---|---|---|
| | $R_m$ [MPa] | $R_{p0.2}$ [MPa] | $A$ [%] | $R_m$ [MPa] | $R_{p0.2}$ [MPa] | $A$ [%] |
| IMV6 | 304 | 242 | 16 | - | - | - |
| MA2-1 | 290 | 220 | 11.9 | 382 | 294 | 7.4 |
| MA15 | 269 | 225 | 11.0 | 397 | 314 | - |
| MA12 | 223 | 153 | 9.5 | 270 | 201 | 9.3 |
| IMV2 or MA21 | 209 | 128 | 6.3 | 308 | 203 | 6.3 |

**Table 10.** Fatigue life $N_0$ and length of fatigue micro-crack initiation $N_i$ at room temperature and −135 °C [28].

| Alloy | Room Temperature | | | −135 °C | | |
|---|---|---|---|---|---|---|
| | $N_0$ [$10^3$ cycles] | $N_i$ [$10^3$ cycles] | $N_i/N_0$ | $N_0$ [$10^3$ cycles] | $N_i$ [$10^3$ cycles] | $N_i/N_0$ |
| IMV6 | 130 | 12 | 0.09 | 530 | 210 | 0.4 |
| MA2-1 | 96 | 9 | 0.09 | 305 | 130 | 0.4 |
| MA15 | 65 | 8 | 0.12 | 200 | 110 | 0.55 |
| MA12 | 30 | 6 | 0.2 | 78 | 35 | 0.45 |
| IMV2 or MA21 | 117 | 8 | 0.08 | 104 | 36 | 0.36 |

## 4. Conclusions

### 4.1. Effects of Cryogenic Treatment

Cryogenically treating magnesium alloys alters their microstructure, and in some cases it is able to improve mechanical properties. This has been explained by the following:

- Changes of microstructure, with more twinning in combination with grain orientation changes [8].
- Increased content of precipitated phases, like $Mg_{17}Al_{12}$, which strengthens the material [9].
- Improvement of ductility due to loss of brittle phases, like $Al_4RE$ at low temperatures [10]. This can also improve corrosion resistance.

An interesting assumption is made in [15]. The contraction which comes along with DCT favors the formation of precipitates that have a much lower atomic density compared to that of the surrounding $\alpha$-Mg. This is intended to be a criterion for further research into DCT with magnesium alloys.

### 4.2. Low Temperature Properties

Magnesium alloys exhibit a high yield and tensile strength at low temperatures. Even at very low temperatures their behavior is still quite ductile. The following explanations are given for increasing strength at decreasing temperatures:

- It is assumed that in magnesium alloys at low temperatures, twinning becomes the rate controlling deformation mechanism rather than slip of dislocations.
- The high solid solubility of the atoms of alloying elements is reduced at lower temperatures, where precipitates form and strengthen the alloy.

A minimum ductility of Li-containing magnesium alloys was found in [20], which may be due to temperature-dependent phase changes from an HCP to BCC structure. For ZM21 alloy, there is a sharp increase in ductility between −17.8 °C and 93 °C, which is considered to be a brittle to ductile transition [22]. The same effect has been found in AZ80 [24] at lower temperatures between −130 °C and −60 °C.

**Conflicts of Interest:** The author declares that he has no conflict of interest.

## References

1. Fenn, R.W. Low-temperature properties of cast and wrought magnesium alloys. *ASTM Special Tech. Publ.* **1961**, *287*, 51–57.
2. Barnett, M.R. Twinning and the ductility of magnesium alloys Part I: "Tension" twins. *Mater. Sci. Eng.* **2007**, *A464*, 1–7. [CrossRef]
3. Barnett, M.R. Twinning and the ductility of magnesium alloys Part II. "Contraction" twins. *Mater. Sci. Eng.* **2007**, *A464*, 8–16. [CrossRef]
4. Bussiba, A.; Kupiec, M.; Ifergane, S.; Stechman, A.; Ben-Artzi, A. Fracture and deformation potential of magnesium alloys at low temperatures. In *CP614, Advances in Cryogenic Engineering: Proceedings of the International Cryogenic Materials Conference*; Balachandran, B., Ed.; CMC: Madison, WI, USA, 2002; Volume 48, pp. 84–91.
5. Baldissera, P.; Delprete, C. Deep cryogenic treatment: A bibliographic review. *Open Mech. Eng. J.* **2008**, *2*, 1–11. [CrossRef]
6. Yang, H.S.; Wang, J.; Shen, B.L.; Liu, H.H.; Gao, S.J.; Huang, S.J. Effect of cryogenic treatment on the matrix structure and abrasion resistance of white cast iron subjected to destabilization treatment. *Wear* **2006**, *261*, 1150–1154. [CrossRef]

7. Bensely, A.; Venkatesh, S.; Mohan Lal, D.; Nagarajan, G.; Rajadurai, A.; Junik, K. Effect of cryogenic treatment on distribution of residual stress in case carburized En 353 steel. *Mater. Sci. Eng.* **2008**, *A479*, 229–235. [CrossRef]
8. Jiang, Y.; Chen, Y.; Chen, Z.; Liu, J. Effect of cryogenic treatment on the microstructure and mechanical properties of AZ31 magnesium alloy. *Mater. Manufact. Proc.* **2010**, *25*, 837–841. [CrossRef]
9. Jiang, Y.; Chen, D.; Jiang, Q. Effect of cryogenic thermocycling treatment on the structure and properties of magnesium alloy AZ91. *Met. Sci. Heat Treatm.* **2012**, *53*, 589–591.
10. Bhale, P.; Shastri, H.; Mondal, A.K.; Masanta, M.; Kumar, S. Effect of deep cryogenic treatment on microstructure and properties of AE42 Mg alloy. *J. Mater. Eng. Perform.* **2016**, *25*, 3590–3598. [CrossRef]
11. Mónica, P.; Bravo, P.M.; Cárdenas, D. Deep cryogenic treatment of HPDC AZ91 magnesium alloys prior to aging and its influence on alloy microstructure and mechanical properties. *J. Mater. Proc. Technol.* **2017**, *239*, 297–302. [CrossRef]
12. Asl, K.M.; Tari, A.; Khomamizadeh, F. Effect of deep cryogenic treatment on microstructure, creep and wear behaviors of AZ91 magnesium alloy. *Mater. Sci. Eng.* **2009**, *A523*, 27–31. [CrossRef]
13. Amini, K.; Akhbarizadeh, A.; Javadpour, S. Investigating the effect of quench environment and deep cryogenic treatment on the wear behavior of AZ91. *Mater. Des.* **2014**, *54*, 154–160. [CrossRef]
14. Liu, Y.; Shao, S.; Xu, C.; Yang, X.; Lu, D. Enhancing wear resistance of Mg–Zn–Gd alloy by cryogenic treatment. *Mater. Lett.* **2012**, *76*, 201–204. [CrossRef]
15. Liu, Y.; Shao, S.; Xu, C.S.; Zeng, X.S.; Yang, X.J. Effect of cryogenic treatment on the microstructure and mechanical properties of Mg–1.5Zn–0.15 Gd magnesium alloy. *Mater. Sci. Eng.* **2013**, *A588*, 76–81. [CrossRef]
16. Dinesh, S.; Senthilkumar, V.; Asokan, P.; Arulkirubakaran, D. Effect of cryogenic cooling on machinability and surface quality of bio-degradable ZK60 Mg alloy. *Mater. Des.* **2015**, *87*, 1030–1036. [CrossRef]
17. Il'ina, I.; Sidorov, N.G.; Morozov, B.S.; Nikitina, M.F.; Koshalev, P.F. The relation between mechanical properties and structure of aluminium and magnesium cast alloys at low temperatures. *Strength Mater.* **1970**, *2*, 1075–1078. [CrossRef]
18. Jiao, X.D.; Li, L.R.; Liu, H.J.; Yang, K. Mechanical properties of low density alloys at cryogenic temperatures. *AIP Conf. Proc.* **2006**, *824*, 69–76.
19. McCammon, R.D.; Rosenberg, H.M. The fatigue and ultimate tensile strengths of metals between 4.2 and 293 K. *Proc. R. Soc.* **1957**, *242*, 203–211. [CrossRef]
20. Martin, H.L.; Imgram, A.G.; Lyman, W.S. *NASA SP-5012 Technology Utilisation Report: Effects of Low Temperature on Structural Metals*; NASA, Technology Utilization Division: Washington, DC, USA, 1964; pp. 27, 28, 53, and 54.
21. Leavenworth, H.W.; Dunkerley, F.J. *Development of Light Weight Magnesium Alloys for Low Temperature Applications*; Final Summary Report; American Machine & Foundry Company: Alexandria, VA, USA, 1967; Contract No. NAS 8–11168.
22. Montana, J.W.; Nelson, E.E. *ZM-21 magnesium alloy corrosion properties and cryogenic to elevated temperature mechanical properties*; NASA Tech. Memo. TM X-64645, George C. Marshall Space Flight Center: Huntsville, AL, USA, 1972.
23. Weiss, V.; Schaeffer, G.T.; Saule, A.; Sachs, G. Thermal cycling under constant load to low temperatures of aluminium and magnesium alloys. *ASTM Special Tech. Publ.* **1961**, *287*, 37–50.
24. Tang, W.; Li, X.; Han, E.; Xu, Y.; Li, Y. Deformation behaviour of AZ80 wrought magnesium alloy at cryogenic temperatures. In *CP824, Advances in Cryogenic Engineering: Trans. of the Int. Cryogenic Materials Conf.-ICMC*; Balachandran, U., Ed.; American Institute of Physics: Melville, NY, USA, 2006; Volume 52, pp. 176–183.
25. Wang, H.; Dong, S.; Lv, G. Plastic deformation characteristics of an Mg–3Al–1Zn alloy at low temperatures. *Mater. Des.* **2016**, *92*, 143–150. [CrossRef]
26. Grinberg, N.M.; Serdyuk, V.A.; Ostapenko, I.L.; Malinkina, T.I.; Kamyshkov, A.S. Effect of low temperature on fatigue failure of magnesium alloy MA12. *Mater. Sci.* **1979**, *15*, 17–21. [CrossRef]
27. Serdyuk, V.A.; Grinberg, N.M.; Malinkina, T.I.; Kamyshkov, A.S. Influence of low temperature on the kinetics of fatigue failure of magnesium alloys. *Mater. Sci.* **1980**, *16*, 63–65. [CrossRef]
28. Sertsyuk, V.A.; Grinberg, N.M.; Ostapenko, I.L. Fatigue fracture of some magnesium alloys in vacuum at room and low temperatures. *Mater. Sci.* **1980**, *15*, 362–365. [CrossRef]

29. Serdyuk, V.A. Fatigue crack growth rate in magnesium alloys at room and low temperatures. *Strength Mater.* **1980**, *12*, 1355–1361. [CrossRef]
30. Grinberg, N.M.; Serdyuk, V.A.; Malinkina, T.I.; Kamyshkov, A.S. Influence of vacuum and low temperature on fatigue crack growth rate in magnesium alloy sheets. *Mater. Sci.* **1983**, *18*, 331–336. [CrossRef]